3-5-2015

THz Fiber Bragg Grating for Distributed Sensing

Zhen Chen
University of Rhode Island

Lei Yuan

Gerald Hefferman

Tao Wei
University of Rhode Island, tao_wei@uri.edu

Citation/Publisher Attribution

Chen Z, Yuan L, Hefferman G, and Wei, T. (2015). THz fiber Bragg grating for distributed sensing. *Photonics Technology Letters, IEEE*, *27*(10), 1084-1087. doi 10.1109/LPT.2015.2407580
Available at: http://dx.doi.org/10.1109/LPT.2015.2407580

THz fiber Bragg grating for distributed sensing

Zhen Chen, Lei Yuan, Gerald Hefferman, and Tao Wei

***Abstract*—This letter reports a fiber Bragg grating for distributed sensing applications fabricated using single-mode optical fiber and a femtosecond laser and interrogated in the terahertz range. A theoretical model of device behavior was derived, which agreed well with experimentally observed device behavior. In order to investigate the utility of terahertz fiber Bragg gratings (THz FBGs) as a sensing modality, temperature tests were conducted. The results demonstrated a sensitivity of -1.32 GHz/ºC and a detection resolution of less than 0.0017 ºC. A temperature distribution test was also conducted using a THz FBG, demonstrating its potential as a distributed sensing platform with high spatial resolution. The feasibility of interrogating THz FBGs using narrow interrogation bandwidths was also experimentally shown.**

***Index Terms*—interferometry, optical fiber sensor**

I. Introduction

The Bragg grating is a mature sensing technique that has been widely used for strain, stress, pressure, and temperature measurement. Through the integration of these periodic structures into a variety of waveguides, the utility of Bragg grating technology has been successfully demonstrated over a broad set of frequency ranges. In the optics domain, incident frequencies in the hundreds of terahertz are routinely used to interrogate fiber Bragg gratings (FBG) [1]. By resolving shifts in the reflected spectra, subtle changes in the parameters of interest can be precisely measured. Similar utility has been demonstrated in the microwave domain (a few gigahertz) through the successful implementation of coaxial cable Bragg gratings (CCBG) fabricated by introducing discontinuities at the centimeter scale [2, 3].

Both FBG and CCBG have demonstrated their utility for large scale, multiplexed sensing applications [4, 5]. However, these techniques have distinct limitations; the large frequency ranges necessary for interrogation in the optical domain require swept frequency lasers, or a combination of broadband light source and optical spectrum analyzer, with broad ranges (tens of nm, or a few terahertz, at a wavelength of around 1550 nm) [6], while the long pitch-length of CCBGs in the microwave domain limits its spatial resolution (~tens of cm) for sensing applications.

Manuscript received Jan. 26, 2015. The research work was supported by the National Science Foundation through Program (CCF-1439011).

Z. Chen and T. Wei are with the Department of Electrical, Computer and Biomedical Engineering, University of Rhode Island, Kingston, RI 02881, USA (e-mail: wei@ele.uri.edu)

L. Yuan is with the Department of Electrical and Computer Engineering, Clemson University, Clemson, SC 29634, USA.

G. Hefferman is with the Warren Alpert Medical School of Brown University, Providence, RI 02903, USA

Terahertz frequency sensing has emerged as a promising method of surmounting the limitations of both the optical and microwave domains. Terahertz frequencies lie between the optical and microwave frequency ranges, which are hundreds of terahertz and tens of gigahertz, respectively. As a consequence of this spectral position, terahertz sensing has the potential to marry the positive qualities of both optical and microwave Bragg grating techniques [7]; as compared to a FBG and CCBG, THz gratings require a narrower interrogation bandwidth (hundreds of gigahertz) and have greater spatial resolution (pitch length < 1 mm), respectively.

This possibility has led to recent promising experimental investigation. Zhou et al., using a KrF laser to modify Topas polymer fiber, interrogated the resulting structure using a high frequency vector network analyzer at hundreds of gigahertz [8]. Similarly, Yan et al. used a CO_2 laser to modify a step-index polymer fiber, testing the structure using terahertz time-domain spectroscopy at hundreds of gigahertz [9]. Both methods, however, suffer from significant insertion loss as a result of large perturbations of the waveguides, which significantly limits the multiplexing capability of resulting sensors. Additionally, the need to interrogate these sensors using direct terahertz frequency modulation requires the use of precision instrumentation at considerable expense due to the high attenuation of the interrogating circuit at THz frequencies.

In this letter, we report a terahertz fiber Bragg grating (THz FBG) sensing modality with the potential to overcome these engineering limitations. By using heterodyne mixing, a mainstay of microwave photonics, this technique has the potential to lead to both simplified sensor interrogation using narrow interrogation bandwidths and greatly-enhanced distributed sensing capacity with high spatial resolution [10-14]. The interrogation system, fabrication parameters, and sensing utility of THz FBGs were experimentally studied, and the results presented in this letter.

II. Operation Mechanism

The schematic of the interrogation system, based on optical frequency domain reflectometry (OFDR), is shown in Fig. 1 [15, 16]. The light generated by the tunable laser source (TLS) is split by a 90/10 optical coupler (CPL) into two paths, “clock” and “signal”. The “clock” path with two 50/50 CPLs is an interferometer that provides the sample clock for the data acquisition card (DAQ), compensating for the non-linearity of the tunable laser. The sampling rate of DAQ is 14 MSa/sec. The light in the “signal” path is split using a 50/50 coupler into a reference arm and a detection arm; a circulator (CIR)

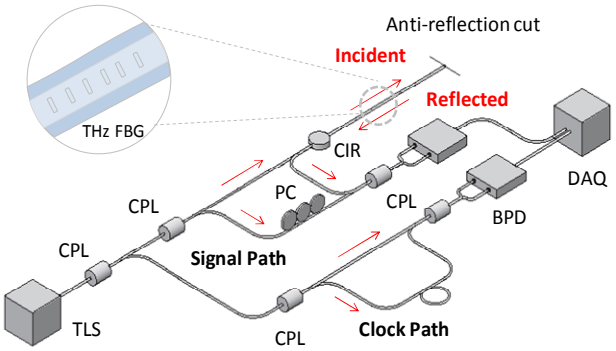

Fig. 1. Schematic of the interrogation system for THz FBG

guides the reflected light from the THz FBG structure, which is terminated with anti-reflected cut; a polarization controller is placed on the reference arm to adjust the interferometer for maximum output; another 50/50 CPL recombines the light from reference arm and detection arm to the balanced photodiodes (BPD) and DAQ. In this setup, the tunable laser sweeps from 1525 to 1555 nm at 60 nm/s scanning speed, corresponding to a total bandwidth of 3.8 THz, resulting in 1066357 sampling points in one waveform. The bandwidth of the tunable laser was reduced to 40 GHz to demonstrate the possibility of using smaller bandwidth for sensor demodulation. The real-time system has an update rate of 1.5 sec per round, which includes 0.5 sec for laser scanning and 1 sec for transmission of the data to a PC and calculation. The coherence length of the tunable laser is around 400 m, limiting the total length of the fiber detection arm to be 400 m.

Fig. 2 illustrates the technique used to fabricate the THz FBGs under experimental investigation. The structures were fabricated with a Ti:Sapphire fs laser (Coherent, Inc.) micromachining system from the single-mode optical fiber (Corning, SFM-28), with core and cladding diameters of 8.2 and 125 µm respectively, for all experimental trials [17-19]. The insertion of each reflector is smaller than 0.001 dB.

A theoretical framework was developed to model the behavior of a multiplexed THz FBG. In this model, M same THz FBGs are embedded along the detection arm, with each FBG containing equally N reflection points with a period of Δz. The total AC coupled voltage received by the DAQ can then be expressed as:

$$v_{total} = 2\eta r I_{ref} \sum_{m=0}^{M-1} \sum_{n=0}^{N-1} \cos\left[\beta\left(z_{ref} - z_m - 2n\Delta z\right)\right] \quad (1)$$

where η is the light-to-voltage conversion coefficient of the photodiode, r is the reflection coefficient of the FBG reflectors, I_{ref} is the light intensity of the reference arm, β is the propagation constant, z_{ref} is the length from the reference arm to the PD, and z_m is the length from the start of the m^{th} FBG to the PD. The intensity of the reflected light can be obtained using a Fourier transform. In this study, Rayleigh scattering is defined as the noise floor, resulting in a signal-to-noise ratio (SNR) of ~ 23 dB. Signal from target FBGs from the fiber under test can be extracted via a Butterworth band-pass filter. The sensing mechanism is based on tracking the frequency shift of the THz FBG signal related with the ambient change. To extract the THz FBG signal shift, a self-mixing technique was applied to the extracted individual THz FBG signal. The reflected signal in frequency domain is squared and filtered using a low-pass filter to obtain the FBG reflection spectrum:

$$S = 2\eta^2 r^2 {I_{ref}}^2 \sum_{i=0}^{N-1} \sum_{j=0}^{N-1} cos[2\beta(i-j)\Delta z] \quad (2)$$

Fig. 3 shows both simulation and experimental results from 1 mm and 0.1 mm THz FBGs. Both structures were fabricated with 20 reflection points using a fs laser at 0.11 W power. Some noise features are evident in the experiment signals, which are attributed to imperfections introduced during fabrication. The simulation results agree well with the experimental data.

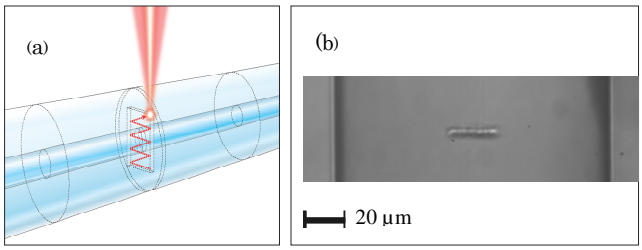

Fig. 2. Fabrication of THz FBG with femtosecond laser

III. Experiments, Results and Discussion

In order to determine the effect of varying the number reflection points on signal quality, the full width at half maximum (FWHM) of signals from gratings with differing numbers of reflectors were measured. Three THz FBGs were fabricated using the same period (1 mm) and same fabrication power (0.11 W), and with 10, 20, and 40 reflection points, respectively. Data were sampled 100 times from each THz FBG. The average FWHM results for the 10, 20, and 40 reflection point THz FBGs were 7.03 GHz, 3.85 GHz, and 1.27 GHz, respectively. These results indicate that, when period and fabrication power are held constant, increasing the number of reflection points of a THz FBG results in enhanced signal quality factor (Q-factor). However, the trade-off is the mitigated spatial resolution due to the increased grating length.

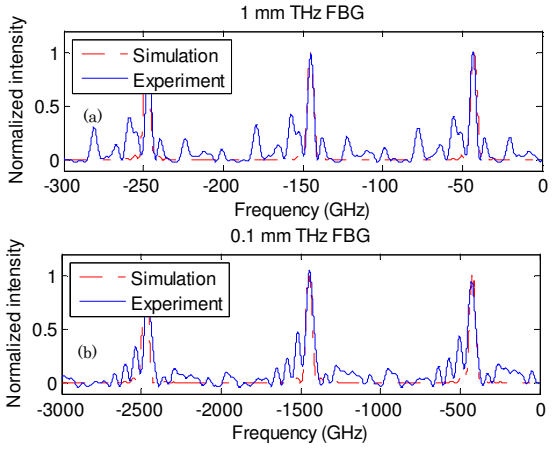

Fig. 3. Simulation and experimental results: (a) 1 mm, 20 reflection points, 0.11 W; (b) 0.1 mm, 20 reflection points, 0.11 W

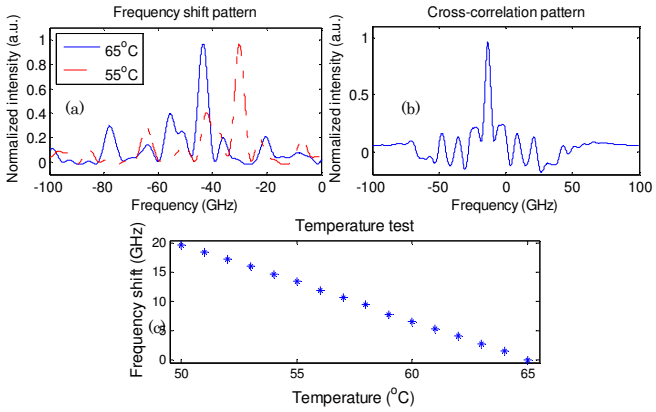

Fig. 4. Temperature response: (a) 1 mm THz FBG reflection spectra at 65 ºC and 55 ºC; (b) cross-correlation pattern to extract the frequency shift from (a); (c) frequency shift as a function of temperature

To investigate the potential utility of a THz FBG as a temperature sensor, a THz FBG was fabricated using a fs laser power of 0.11 W, a period length of 1 mm, and 20 reflection points. The THz FBG was placed in a temperature-controlled water bath and the sensor's temperature response measured. Fig. 4 (a) shows the THz FBG frequency signal at both 55 ºC and 65 ºC. As the temperature increases, the period of FBG increases, causing a corresponding shift in resonant frequency. The frequency shift can be extracted by calculating the cross correlation pattern. Fig. 4(b) shows the normalized cross-correlation pattern from Fig. 4(a) with a frequency shift of 12.84 GHz. Fig. 4(c) plots the temperature response from 50 ºC to 65 ºC. Using this configuration, the temperature sensitivity for the THz FBG was observed to be approximately -1.32 GHz/ºC. It is worth noting that the sensitivity of THz FBG is much larger than conventional microwave grating due to the fact that the interrogation window in the proposed setup is in optical range, and the grating resonant peak under test is at a much higher order in comparison with 1st order in a microwave grating. For 1 mm grating, the resonant peaks range from 1923th to 1967th order, given that the laser tuning bandwidth is from 1525 to 1555 nm.

In order to investigate the distributed sensing capability of the system, a 40 reflection point THz FBG was fabricated with a period of 1 mm, shown in Fig. 5(a). The system was calibrated using the reflectivity of an APC connector, which

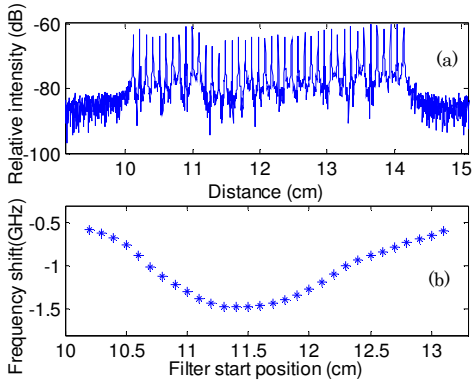

Fig. 5. Distributed sensing test with THz FBG array: (a); a time-domain 40 reflection point THz FBG signal; (b) frequency-shift distribution measured using THz FBG array [Media 1].

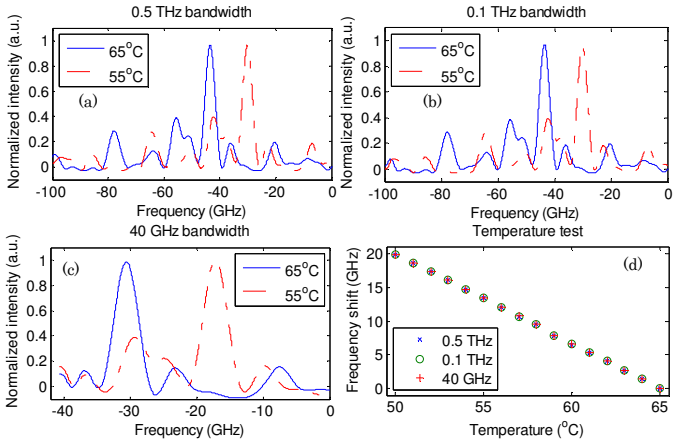

Fig. 6. Temperature response of 1mm THz FBG using different laser sweeping ranges: (a) - (c) temperature response with 3 interrogation bandwidth, (d) temperature test with different interrogation bandwidth

was previously measured to be -60 dB using precision instrument. The reflectivity of each point is around -70 dB. The reflectivity of each reflection point varies due to imperfections in the fabrication process. The reflection spectra of THz FBG were first measured with no temperature change as reference. An ice cube was then placed ~1 cm away from the THz FBG close to center in order to introduce a temperature distribution along the fiber sensor. The spectra were again taken and a high order 0.1 ns time-domain moving filter, corresponding to 1 cm in spatial domain, was used to gate the FBG signal with a step of 1 mm. 90% of the filter window was overlapped with its neighboring filter window. The frequency shift as a function of filter start position was plotted in Fig. 5(b). A Gaussian-like temperature distribution was observed in which the center THz FBG experienced a frequency shift corresponding to a temperature approximately 1 ºC lower than that of either edge of the THz FBG sensor. A real-time experimental demo was videotaped and attached to this letter. This experiment demonstrates that THz FBGs hold the potential for continuous distributed sensing with high spatial resolution. In addition, the ultraweak reflection nature of so fabricated THz FBGs promises a huge multiplexing capacity [20].

A key feature of THz FBGs is that they require a much narrower detection bandwidth than FBGs in the optical frequency range while maintaining good spatial resolution. To demonstrate this feature, a THz FBG with 20 reflection points was tested using differing sweeping bandwidths from a tunable laser. Fig. 6 (a-c) shows the spectra of the sensor under test using these differing laser sweep bandwidths. Fig. 6 (d) shows the temperature response for each different bandwidth, which are observed to agree well with each other. These results demonstrate that, when compared with a conventional optical FBG, use of a THz FBG can effectively reduce detection bandwidth.

To evaluate system-level accuracy, a stability test was conducted by fixing the temperature of a 1 mm, 20 reflection point THz FBG. 100 spectra were recorded using this configuration. The frequency shift of each spectrum relative to its initial status was calculated. The standard deviation of the

frequency shift was less than 2.27 MHz. Given the experimentally measured sensitivity of -1.32 GHz/ºC, its temperature detection limit is calculated to be less than 0.0017 ºC. This demonstrates that THz FBG holds significant potential for high-accuracy detection. The temperature sensing dynamic range is limited by the free spectral range (FSR) of THz FBGs. Frequency shift beyond FSR will result in spectral ambiguity problem. For example, 1 mm THz FBG has a FSR of ~100 GHz, corresponding to a dynamic range of ~76˚C. The dynamic range is inversely proportional to the pitch length of THz FBG. In addition, large dynamic range requires wide interrogation bandwidth.

IV. Conclusion

To conclude, this letter reports the development of a FBG operating in the terahertz range with the demonstrated potential to combine the high spatial resolution of FBGs with the narrow detection bandwidth of CCBGs. The effect of varying the number of reflectors on signal quality was quantified. The potential of a THz FBG as a temperature sensor was experimentally validated, with a sensitivity of -1.32 GHz/ºC and a detection resolution of less than 0.0017 ºC. The utility of THz FBGs for distributed sensing with high spatial resolution was experimentally demonstrated. Similarly, differing interrogation bandwidths (0.5 THz, 0.1 THz, and 40 GHz) were shown, in Fig. (6), to have identical temperature sensitivities, illustrating that THz FBGs can be successfully interrogated using narrower bandwidths than current optical FBGs.

References

[1] K. O. Hill and G. Meltz, "Fiber Bragg grating technology fundamentals and overview," *Journal of lightwave technology,* vol. 15, pp. 1263-1276, 1997.

[2] T. Wei, S. Wu, J. Huang, H. Xiao, and J. Fan, "Coaxial cable Bragg grating," *Applied Physics Letters,* vol. 99, p. 113517, 2011.

[3] S. Wu, T. Wei, J. Huang, H. Xiao, and J. Fan, "Modeling of Coaxial Cable Bragg Grating by Coupled Mode Theory," *Transactions on Microwave Theory and Techniques, IEEE Transactions on,* vol. 62, pp. 2251-2259, 2014.

[4] Y. Wang, J. Gong, B. Dong, D. Y. Wang, T. J. Shillig, and A. Wang, "A Large Serial Time-Division Multiplexed Fiber Bragg Grating Sensor Network," *Lightwave Technology, Journal of,* vol. 30, pp. 2751-2756, 2012.

[5] J. Huang, T. Wei, X. Lan, J. Fan, and H. Xiao, "Coaxial cable Bragg grating sensors for large strain measurement with high accuracy," in *SPIE Smart Structures and Materials+ Nondestructive Evaluation and Health Monitoring*, 2012, pp. 83452Z-83452Z-9.

[6] A. D. Kersey, M. A. Davis, H. J. Patrick, M. LeBlanc, K. P. Koo, C. G. Askins, M. A. Putnam, and E. J. Friebele, "Fiber grating sensors," *Journal of Lightwave Technology,* vol. 15, pp. 1442-1463, Aug 1997.

[7] P. H. Siegel, "Terahertz technology in biology and medicine," in *Microwave Symposium Digest, 2004 IEEE MTT-S International*, 2004, pp. 1575-1578.

[8] S. F. Zhou, L. Reekie, H. P. Chan, Y. T. Chow, P. S. Chung, and K. Man Luk, "Characterization and modeling of Bragg gratings written in polymer fiber for use as filters in the THz region," *Optics Express,* vol. 20, pp. 9564-9571, 2012.

[9] G. Yan, A. Markov, Y. Chinifooroshan, S. M. Tripathi, W. J. Bock, and M. Skorobogatiy, "Resonant THz sensor for paper quality monitoring using THz fiber Bragg gratings," *Optics letters,* vol. 38, pp. 2200-2202, 2013.

[10] J. Huang, X. Lan, T. Wei, Q. Han, Z. Gao, Z. Zhou, and H. Xiao, "Radio frequency interrogated actively mode-locked fiber ring laser for sensing application," *Optics Letters,* vol. 37, pp. 494-496, 2012.

[11] T. Wei, J. Huang, X. Lan, Q. Han, and H. Xiao, "Optical fiber sensor based on a radio frequency Mach–Zehnder interferometer," *Optics Letters,* vol. 37, pp. 647-649, 2012.

[12] J. Huang, L. Hua, X. Lan, T. Wei, and H. Xiao, "Microwave assisted reconstruction of optical interferograms for distributed fiber optic sensing," *Optics Express,* vol. 21, pp. 18152-18159, 2013.

[13] J. Huang, L. Hua, X. Lan, and H. Xiao, "Fiber optic distributed sensing technology based on microwave reconstructed optical interferograms," in *Frontiers in Optics 2013 Postdeadline*, Orlando, Florida, 2013, p. FW6B.1.

[14] J. Huang, X. Lan, M. Luo, and H. Xiao, "Spatially continuous distributed fiber optic sensing using optical carrier based microwave interferometry," *Optics Express,* vol. 22, pp. 18757-18769, 2014/07/28 2014.

[15] Z. Chen, L. Yuan, G. Hefferman, and T. Wei, "Ultra-weak intrinsic FP cavity array for distributed sensing," *Optics Letters,* 2014.

[16] Z. Chen, Y. Zeng, G. Hefferman, Y. Sun, and T. Wei, "FiberID: Molecular-level secret for identification of things," in *IEEE Workshop on Information Forensics and Security (WIFS'14), Altalanta GA, Dec 3-5 2014*, 2014.

[17] Y. Zhang, L. Yuan, X. Lan, A. Kaur, J. Huang, and H. Xiao, "High-temperature fiber-optic Fabry–Perot interferometric pressure sensor fabricated by femtosecond laser," *Optics Letters,* vol. 38, pp. 4609-4612, 2013.

[18] L. Yuan, T. Wei, Q. Han, H. Wang, J. Huang, L. Jiang, and H. Xiao, "Fiber inline Michelson interferometer fabricated by a femtosecond laser," *Optics Letters,* vol. 37, pp. 4489-4491, 2012.

[19] L. Yuan, J. Huang, X. Lan, H. Wang, L. Jiang, and H. Xiao, "All-in-fiber optofluidic sensor fabricated by femtosecond laser assisted chemical etching," *Optics Letters,* vol. 39, pp. 2358-2361, 2014.

[20] W. Yunmiao, G. Jianmin, D. Y. Wang, D. Bo, B. Weihong, and W. Anbo, "A Quasi-Distributed Sensing Network With Time-Division-Multiplexed Fiber Bragg Gratings," *Photonics Technology Letters, IEEE,* vol. 23, pp. 70-72, 2011.